HUMAN GENE THERAPY 24:508–519 (May 2013)

DOI: 10.1089/hum.2012.158

Research Articles

Hepatic Stellate Cell–Targeted Delivery of Hepatocyte Growth Factor Transgene via Bile Duct Infusion Enhances Its Expression at Fibrotic Foci to Regress Dimethylnitrosamine-Induced Liver Fibrosis

Balakrishnan Chakrapani Narmada,[1–4,*] Yuzhan Kang,[5,*] Lakshmi Venkatraman,[2,6] Qiwen Peng,[3,6] Rashidah Binte Sakban,[4] Bramasta Nugraha,[1–3] Xuan Jiang,[7] Ralph M. Bunte,[8] Peter T.C. So,[5,6,9,10] Lisa Tucker-Kellogg,[2,6] Hai-Quan Mao,[7] and Hanry Yu[1–6,10,*]

Abstract

Liver fibrosis generates fibrotic foci with abundant activated hepatic stellate cells and excessive collagen deposition juxtaposed with healthy regions. Targeted delivery of antifibrotic therapeutics to hepatic stellate cells (HSCs) might improve treatment outcomes and reduce adverse effects on healthy tissue. We delivered the hepatocyte growth factor *(HGF)* gene specifically to activated hepatic stellate cells in fibrotic liver using vitamin A–coupled liposomes by retrograde intrabiliary infusion to bypass capillarized hepatic sinusoids. The antifibrotic effects of DsRed2-HGF vector encapsulated within vitamin A–coupled liposomes were validated by decreases in fibrotic markers *in vitro*. Fibrotic cultures transfected with the targeted transgene showed a significant decrease in fibrotic markers such as transforming growth factor-β1. In rats, dimethylnitrosamine-induced liver fibrosis is manifested by an increase in collagen deposition and severe defenestration of sinusoidal endothelial cells. The HSC-targeted transgene, administered via retrograde intrabiliary infusion in fibrotic rats, successfully reduced liver fibrosis markers alpha-smooth muscle actin and collagen, accompanied by an increase in the expression of DsRed2-HGF near the fibrotic foci. Thus, targeted delivery of *HGF* gene to hepatic stellate cells increased the transgene expression at the fibrotic foci and strongly enhanced its antifibrotic effects.

Introduction

Fibrosis progression is marked by the activation of quiescent hepatic stellate cells (HSCs) and portal fibroblasts into myofibroblasts that occurs due to changes in soluble factors, extracellular matrix (ECM) proteins, and mechanical stiffness (Bataller and Brenner, 2005; Olsen *et al.*, 2011). Activated myofibroblasts secrete copious amounts of ECM proteins, especially collagens that accumulate to form fibrous tissue (Kisseleva and Brenner, 2007). Fibrotic foci are active fibrotic sites within the affected organ (Scotton and Chambers, 2007) with high numbers of activated myofibroblasts, creating a concentrated center of profibrotic cytokines, such as transforming growth factor-β1 (TGF-β1), and accumulation of ECM proteins such as collagen I.

Antifibrotic therapies lacking cell specificity fail to target the fibrotic foci and lead to adverse effects in healthy nonspecific cells surrounding the foci, affecting their viability, differentiated state, and metabolic function (Fallowfield, 2011; Poelstra *et al.*, 2011; Schuppan and Pinzani, 2012). Recent interest in the development of therapeutics targeted to fibrotic foci aims to reduce both the therapeutic dose and the

[1]NUS Graduate School for Integrative Science and Engineering; National University of Singapore, Singapore 117456, Republic of Singapore.
[2]Mechanobiology Institute, Temasek Laboratories; National University of Singapore, Singapore 117411, Republic of Singapore.
[3]Institute of Bioengineering and Nanotechnology, Agency for Science, Technology and Research (A*Star), Singapore 117599, Republic of Singapore.
[4]Department of Physiology; National University of Singapore, Singapore 138669, Republic of Singapore.
[5]Singapore-MIT Alliance for Research and Technology, Singapore 138602, Republic of Singapore.
[6]Singapore-MIT Alliance, Singapore 117576, Republic of Singapore.
[7]Department of Materials Science and Engineering, Johns Hopkins University, Baltimore, MD 21218-2681.
[8]Department of Pathology, Duke-NUS Graduate Medical School, Singapore 169857, Republic of Singapore.
Departments of [9]Mechanical Engineering and [10]Biological Engineering, Massachusetts Institute of Technology, Cambridge, MA 02139.
*These authors contributed equally to this work.

need for long-term therapeutic expression/engraftment efficiency. These antifibrotic therapeutics have targeted HSCs, focusing on eliminating activated HSCs or inhibiting their TGF-β1 signaling/collagen production (Shek and Benyon, 2004; Sato *et al.*, 2008), but these therapeutics neglected the immense synthetic/metabolic capability of myofibroblastic HSCs to facilitate hepatic regeneration. This led us to investigate HSC-targeted hepatocyte growth factor (HGF) therapy to control the expansion of the fibrotic foci, to ameliorate the hepatocellular damage, and to stimulate hepatic regeneration.

HGF, a well-established hepatotrophic factor (Ishiki *et al.*, 1992), has demonstrated antifibrotic effects via suppression of *TGF-β1* and *collagen III* expression (Inoue *et al.*, 2003; Jiang *et al.*, 2008; Kanemura *et al.*, 2008). HSCs are one of the major sources of HGF in the liver, under normal and regenerative conditions (Hu *et al.*, 1993), but sustained activation of HSCs during fibrosis significantly decreases HGF production and inhibits hepatocyte regeneration (Ebrahimkhani *et al.*, 2011). Therefore, we investigated whether targeted delivery of the *HGF* gene to HSCs will yield selective enrichment of the therapeutic transgene in the fibrotic foci leading to a decrease in the number of activated HSCs and collagen accumulation at fibrotic foci. Although the therapeutic strategy aimed at selective enrichment of the therapeutic at the fibrotic foci, the acute changes in hepatic sinusoids during fibrosis pose the risks of obstruction of the sinusoids and increased portal hypertension (DeLeve, 2007). When compared to portal vein infusion, retrograde intrabiliary infusion has several advantages, such as reducing contact with Kupffer cells, increased delivery to the liver, and significant increases in the transgene expression (Otsuka *et al.*, 2000; Dai *et al.*, 2006). To circumvent the damaged hepatic microvasculature and increase the delivery efficacy to the fibrotic liver, we administered the HSC-targeted therapeutic complexes through retrograde intrabiliary infusion.

We used the retinol-storing function of HSCs as a mechanism for targeting HSC, as they are the only liver cells with retinol-storing capability and high expression levels of retinol-binding proteins (Sato *et al.*, 2008; Poelstra and Schuppan, 2011). The antifibrotic potential of the vitamin A–liposome particles containing *HGF* transgene was tested in HSC-T6 (rat hepatic stellate cell line) monoculture, HSC-T6/hepatocyte coculture, and in dimethylnitrosamine (DMN)-induced fibrotic rat livers to test our hypothesis that administering targeted transgene complex will markedly increase the delivery efficiency to HSCs/fibrotic foci and improve therapeutic efficiency.

Materials and Methods

Construction of pDsRed2-HGF plasmid

Rat mRNA was isolated from freshly isolated hepatocytes, and the mRNA was converted to cDNA using an *HGF* gene-specific primer (*HGF* reverse primer in Table 1). The *HGF* gene was isolated using highly specific primers (Table 1) in a polymerase chain reaction (PCR) using Phusion DNA polymerase at primer melting temperature 62°C. The PCR product was run on a 0.8% agarose gel. The band observed near the 2000-bp mark was extracted, purified, and expanded using pJET1.2 cloning vector (Fermentas) and TOP10 cells (Invitrogen). The purified plasmid sequence was verified using HGF-specific sequencing primers designed in-house using Oligo7 software (Table 1; sequencing primers). The *HGF* gene and pDsRed2-C1 ("pDsRed2") vector was restriction-digested using KpnI and BamHI restriction enzymes (NEBL) and ligated using T4 DNA ligase (Promega) cloned into TOP10 competent cells for expansion. Again, the gene sequence was confirmed against the rat *HGF* gene sequence and this purified *pDsRed2-HGF* vector was used for further experiments.

Encapsulation of pDsRed2-HGF construct in vitamin A–coupled liposomes

Liposomes (Lipotrust SR™; Hokkaido System Sciences) were coated with Vitamin A (Retinol; Sigma), as in Sato *et al.* (2008), and purified by dialysis with MWCO 500 membranes (Spectra/Por) for 3 days. The Vitamin A–coupled liposomes were lyophilized using FreeZone from Labconco. The plasmid DNA was encapsulated with the liposomes at the N:P ratio of 11.5:1. The plasmid DNA:Liposome particle size was determined by particle size analyzer to be $\sim$600 nm (data not shown).

In vitro *cultures*

HSC-T6 cells (kindly gifted by Dr. Scott L. Friedman and Dr. Lang Zhuo) were seeded at 2×10^5 cells/35-mm collagen-coated dish (Iwaki) and cultured for 3 days in Dulbecco's modified Eagle's medium (DMEM) with 10% fetal bovine serum (FBS; Sigma) to allow for activation. On the fourth day, the HSC-T6 monoculture was transfected with different liposome/DNA complexes. The HSC-T6/hepatocyte coculture was established with hepatocytes and HSC-T6 cells at the ratio of 1:10 (1 hepatocyte/10 hepatic stellate cells) (Narmada *et al.*, 2012). Four days after HSC-T6 activation, primary rat hepatocytes in an appropriate number to obtain 1:10 ratio were seeded in Williams E (Sigma) with 10% FBS (primary rat hepatocytes were isolated as described previously in Seglen, 1976; the isolation procedure was approved by the National University of Singapore Institutional Animal Care and Use Committee [NUS IACUC]).

The fibrotic cultures were transfected with vitamin A–coupled empty cationic liposomes (VAL) (Lipotrust SR™; Hokkaido System Sciences), or vitamin A–coupled liposomes with pDsRed2 plasmid (VALD), or vitamin A–coupled liposomes with pDsRed2-HGF plasmid (VALH) at the dose of 3-μg plasmid DNA/well. Media was changed 4 hr after transfection. Cell culture supernatants were collected 24 hr after treatment, and the cells were then lysed for RNA isolation.

Transgene validation by transfection in HEK-293T cells

HEK-293T cells were seeded at 5×10^5 cells/35-mm culture dishes in DMEM with serum. One day later, transfection was carried out with 1-μg plasmid DNA using Lipofectamine LTX reagent (Invitrogen) according to the manufacturer's protocol. Media was changed 4 hr after transfection, and the samples were collected 24 hr after transfection.

Measurement of hepatocyte proliferation

The isolated hepatocytes were seeded at 2×10^5 cells/35-mm collagen-coated dish in Williams E with 10% FBS. After 4 hr, media was changed to Williams E without serum.

Table 1. List of Primer Sequences

Gene name	*Primer sequence*
Sequencing primers	
HGF 823 forward	5′ CCGAGGCCATGGTGCTAC 3′
HGF 218 reverse	5′ TCACTTTTTTGGTTTTAAT CTTCAC 3′
HGF 1614 reverse	5′ AAGAACCCAACTTTCCTTTATCA ATG 3′
GAPDH	
Forward	5′ AGACAGCCGCATCTTCTTGT 3′
Reverse	5′ TGATGGCAACAATGTCCACT 3′
HGF	
Forward	5′ AGGTACCGAACTGCAAGCATG 3′
Reverse	5′ GATCCTATGGCTATTA CAACTTGTATGTC 3′
Collagen IV	
Forward	5′ GCAGGTGTGCGGTTTGTGAAG 3′
Reverse	5′ AGCTCCCCTGCCTTCAAGGTG 3′
TIMP-1	
Forward	5′ GCCTACACCCCAGCCATGGA 3′
Reverse	5′ CGGCCCGCGATGAGAAAC 3′

HGF, hepatocyte growth factor; *GAPDH*, glyceraldehyde 3-phosphate dehydrogenase; *TIMP-1*, tissue inhibitors of matrix metalloproteinase-1.

After overnight serum starvation, the cells were treated with filtered conditioned media from transfected HSC-T6 monoculture. Cell lysates were prepared by treatment with 0.1% sodium dodecyl sulphate (SDS), followed by needle homogenization and centrifugation at 11,000 × *g* for 10 min. The supernatant was diluted 10-fold, and the DNA quantity was assayed by incubation with an equal amount of picogreen dsDNA dye for 5 min, fluorescence was measured at 520 nm, and a standard curve was used to calculate the number of cells from the observed DNA quantity.

DMN-induced liver disease

Male Wistar rats (250 g) were administered 1% N-nitrosodimethyl amine (10 mg/kg; Wako) intraperitoneally for 3 consecutive days each week for 4 weeks to establish liver fibrosis. Fresh samples from the right lobe of rat livers were collected and frozen immediately in liquid nitrogen for further RNA and protein analysis. Simultaneously, right-lobe liver sections were fixed in 3.7% phosphate-buffered formaldehyde and processed for histopathology. Blood was collected from the heart by cardiac puncture, centrifuged at 2,000 rpm for 15 min, and the isolated blood serum was stored at −80°C until further processing.

Retrograde intrabiliary infusion

Fibrotic rats were prepared by administering DMN (Kanemura *et al.,* 2008) for 3 consecutive weeks and then not administering DMN for the next 7 days. The protocol for retrograde intrabiliary infusion was adapted from our previous work (Jiang *et al.,* 2007). Rats were anaesthetized with ketamine/xylazine, the common bile duct was canulated with a 32G needle (Hamilton), and a tie with 5-O silk sutures was placed to secure the needle. Liposomes with pDsRed2-HGF (Lip-HGF) or VALD or VALH (200-μg plasmid DNA) were administered at a constant flow rate of 0.2 ml/min through the needle, fitted through Ext-12 tubes (DiLab) over 20 min. After retrograde infusion, a tie was placed between the canulated region of the common bile duct and the liver for 10 min to prevent immediate backflow. After the needle and ties were removed, the abdominal wall of the operated rats was sutured with 3-O-prolene sutures, and the rats were administered Baytril and Buprenorphine for 3 days after surgery. One or 7 days after retrograde infusion, the livers were perfused with 1× sterile PBS and then with 3.7% formaldehyde, and the samples were collected for further processing. All animal procedures were humanely carried out under the premises of the IACUC protocol (090492) approved by the Biological Resource Centre, Biopolis, Singapore.

Real-time PCR for gene expression analysis

The mRNA was isolated from the cells or homogenized tissues using RNeasy mini kit (Qiagen); 1 μg of isolated mRNA from each sample was converted to cDNA (Superscript Reverse Transcriptase III; Invitrogen) and real-time PCR (RT-PCR) reaction (Sybr Green Master mix; Roche) was carried out for *HGF*, alpha-smooth muscle actin (*α-SMA*), collagen I (*Col I*), collagen IV (*Col IV*), *TGF-β1*, thrombospondin-1 (*TSP-1*), plasminogen activator inhibitor-1 (*PAI-1*), tissue inhibitor of metalloproteinases-1 (*TIMP-1*), *β-actin*, and glyceraldehyde 3-phosphate dehydrogenase (*GAPDH*); primer sequences are listed in Table 1 and some are adapted from our previous work (Narmada *et al.,* 2012). The fold change in gene expression values were determined by the Del-Del C_T relative quantitation method (van't Veer *et al.,* 2006); the target C_T values were normalized to the endogenous reference *β-actin* (for *in vitro* cell lysates) and *GAPDH* (for tissue homogenates).

Active TGF-β1 ELISA

For cell culture supernatants, equal volumes of sample were assayed for active TGF-β1 ELISA (Promega TGF-β1 Emax Immunoassay) (Budinger *et al.,* 2006) according to the manufacturer's protocol. For blood samples, protein levels were quantified using the Bradford assay (BioRad), and equal amounts were assayed for active TGF-β1 levels.

Western blots

Conditioned media from transfected cells or tissue homogenates (tissue homogenates lysed in radioimmunoprecipitation assay (RIPA) buffer and protease inhibitor cocktail, P8340; Sigma) were centrifuged at 14,000 rpm at 4°C for 15 mins, protein levels in the supernatant were quantified, and equal amounts of protein samples were separated on a 10% SDS PAGE in 1× Tris Glycine and transferred onto a 0.22 μm nitrocellulose membrane overnight in 1× Tris-buffered saline (TBS) with 10% methanol. The membrane was then treated with blocking buffer (2% skim milk in 1× TBS with 0.01% Tween 20 [1× TBST]) for 1 hr. Later the membrane was washed three times in 1× TBST; treated with mouse α-SMA antibody (Sigma; 1:200), mouse β-actin antibody (Sigma; 1:40000), or goat HGF antibody (Santacruz; 1:100) in 1× TBST for 2 hr; washed three times in 1× TBST; and treated with goat anti-mouse immunoglobulin G–horseradish peroxidase (IgG-HRP) (Santacruz; 1:10000 in blocking buffer) or mouse

anti-goat antibody (Santacruz; 1:10000 in blocking buffer) for 1 hr. The membrane was developed using SuperSignal West Pico Chemiluminescent solution (Thermo Scientific).

Liver protein levels

Liver proteins such as alanine transaminase, aspartate aminotransferase, lactate dehydrogenase, and albumin in the blood serum were quantified with Vitros DT kits using Johnson & Johnson DT 60 analyzer.

Histopathology

Deparaffinized formalin-fixed liver tissue sections of 5 μm thickness were stained with Masson's Trichrome, and the next serial section with Haematoxylin & Eosin, to determine the levels of necrosis, collagen, and Knodell score.

Immunofluorescence imaging

Serial sections from the treated rat livers were deparaffinized, permeabilized, and treated with blocking buffer (5% bovine serum albumin) followed by treatments with primary antibodies for α-SMA (Sigma); TGF-β1 (Santacruz); Collagen I (Millipore), HGFα (Santacruz); DsRed2 (Santacruz); platelet endothelial cell adhesion molecule-1, PECAM-1 (Abcam); von Willebrand Factor, vWF (Santacruz); and hyaluronic acid receptor, CD44 (Abcam). Later, the tissue sections were incubated with appropriate secondary antibodies (Alexafluor; Invitrogen) for 2 hr. After washing, the stained tissue sections were imaged at the portal and the capsular regions with Olympus FluoView FV1000 confocal laser scanning microscope. Marker intensity and colocalizated points were quantified using ImageJ software.

Nonlinear microscopy and image acquisition for collagen

Deparaffinized, unstained liver tissue sections of 50-μm thickness were imaged with second harmonic generation microscopy (SHG) using a modified Carl Zeiss LSM 510 system as described previously (Tai *et al.,* 2009). Data was acquired using both two-photon excited fluorescence and SHG imaging modes. A total of four images (3 × 3 tile scans, 3072 × 3072 pixels, and 3.2 μs well time) were collected for each tissue specimen, and two specimens were extracted from each animal. The SHG images were analyzed using the direct segmentation method (Gaussian mixture model). The method is based on the assumption that the distribution of intensities is a mixture of several Gaussian distributions, each corresponding to a separate tissue class. In an SHG image, the intensity of pixels is modeled as the mixture of two Gaussian distributions, one representing collagen area with strong SHG signals and the other representing the background.

Scanning electron microscopy for sinusoidal endothelial cells

Liver tissue sections (precision cut to 1 mm × 1 mm × 1 mm size) were fixed with 2.5% glutaraldehyde in 0.1 *M* sodium cacodylate buffer overnight and stained with 1% osmium tetroxide for 1 hr. The stained tissue sections were then dehydrated stepwise with ethanol gradient for 10 min each and vacuum dried overnight (Wisse *et al.,* 2010). After gold sputter coating, liver sinusoids were imaged using field emission scanning electron microscopy (FE-SEM; JEOL JSM-6701F) at 10 kV.

Statistical analyses

Statistical analyses were performed using Graphpad Prism 5 software. The results are expressed as mean ± SEM. For all *in vitro* experiments, n = 4; for all animal studies, n ≥ 5. Comparisons between two different groups were performed with unpaired Student's t-test. Differences were considered significant when the p-value < 0.05. Comparisons between three groups were performed with one-way analysis of variance (ANOVA) and Tukey's multiple comparison test. Differences were considered significant when the p-value < 0.05.

Results

pDsRed2-HGF gene construction & in vitro *validation*

The *HGF* gene was isolated from rat cDNA and incorporated into the pDsRed2C1 vector to enable visualization of the delivered gene (Fig. 1A). In order to validate the expression and functionality of the transgene, HEK-293T cells were transfected with pDsRed2 empty vector or with the pDsRed2-HGF construct, and both transfections produced high levels of DsRed2 fluorescence (Fig. 1B). Cells transfected with the pDsRed2-HGF construct expressed significantly higher levels of the *HGF* gene (Fig. 1C), HGF, and DsRed2 proteins (Fig. 1D) compared to the cells transfected with pDsRed2 empty vector. To evaluate the transgene function, primary rat hepatocytes were treated with conditioned media from transfected cells and assessed for proliferation. The media from pDsRed2-HGF-transfected cells was significantly more hepatotrophic than cells transfected with empty vector (Fig. 1E).

Effects of vitamin A-liposome-HGF on fibrotic cultures in vitro

The pDsRed2 empty vector and pDsRed2-HGF constructs were encapsulated in vitamin A–coupled liposomes by gentle mixing for 1 hr at 4°C. HSC-T6 cells (Fig. 2A) were transfected with the prepared VALD or VALH complexes. VALH-treated HSCs secreted significantly higher HGF protein compared to VALD-treated HSCs (Fig. 2B). Conditioned media from VALH-treated HSCs was significantly more hepatotrophic toward primary rat hepatocytes (Fig. 2C). Therefore, VALH particles were effectively taken up by HSC-T6 cells, and the transfected cells produced significant levels of functional HGF.

To assess the antifibrotic effects of VALH particles, we measured the concentration of active TGF-β1 protein and observed a strong decrease in the levels of active TGF-β1 in VALH-treated HSC-T6 monoculture (Fig. 2D). For a more representative fibrotic configuration (Narmada *et al.,* 2012), we employed a coculture of primary rat hepatocytes and HSC-T6 cells at 1:10 ratio (Fig. 2E) and transfected them with the VALD/VALH particles. We measured the expression of several fibrotic genes by RT-PCR, and found significant decreases in the expression levels of *α-SMA, Col I, Col IV, TGF-β1, TSP-1, PAI-1,* and *TIMP-1* in VALH-transfected coculture

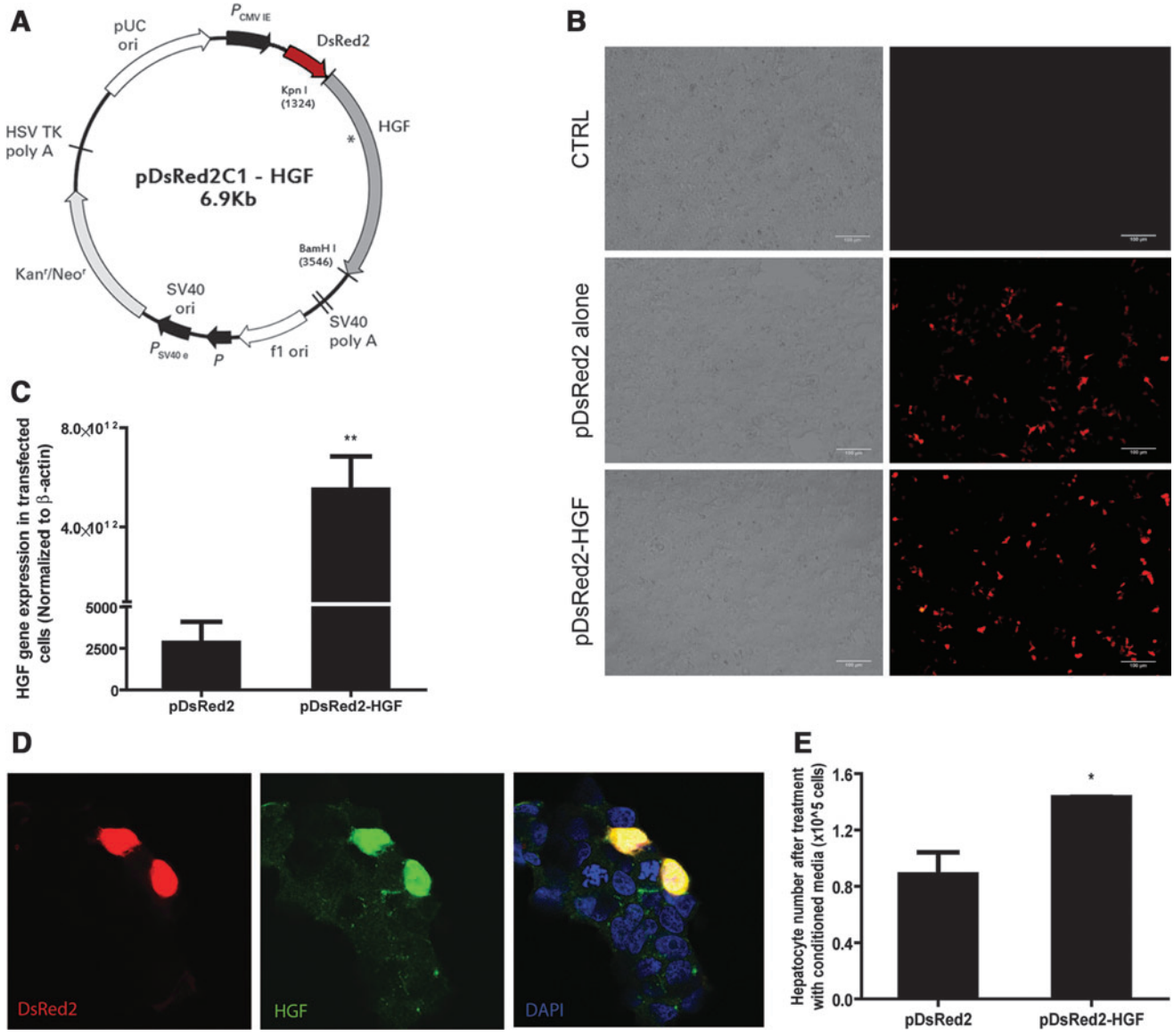

FIG. 1. pDsRed2–hepatocyte growth factor (*HGF*) transgene construction and *in vitro* validation. Vector diagram of *pDsRed2-HGF* transgene construct **(A)**. HEK-293T cells transfected with pDsRed2 or pDsRed2-HGF plasmid DNA **(B)** show DsRed2 autofluorescence. Significant increase in *HGF* gene expression with the transfection of pDsRed2-HGF construct in HEK-293T cells, normalized to *β*-actin **(C)**. Colocalization of DsRed2 and HGF proteins in transfected cells **(D)**. Functional test for secreted HGF protein showed significant increase in primary rat hepatocyte proliferation (Picogreen assay) with conditioned media from pDsRed2-HGF-transfected cells **(E)**. $^*p < 0.05$, $^{**}p < 0.01$.

than in VALD-transfected coculture (Fig. 2F; normalized to *β*-actin). VALH-transfected coculture also showed decreased active TGF-*β*1 levels (Fig. 2G). In summary, the VALH particles demonstrated the ability to reduce the levels of fibrotic factors *in vitro*.

Establishment of DMN-induced liver fibrosis

In order to induce liver fibrosis, male Wistar rats were injected with 1% DMN. DMN-induced fibrotic rats exhibited a high degree of hepatic necrosis, as seen in Masson's trichrome staining (Fig. 3A and B), and an increase in collagen deposition as seen in SHG microscopy of liver tissue sections (Supplementary Fig. S1A and B; Supplementary Material available online at www.liebertonline.com/hum). The Knodell score calculated from tissue histology showed a steep increase between weeks 2 and 4 (Supplementary Fig. S1C). Gene expression profiles of fibrotic factors *α-SMA*, *Col I*, *Col IV*, *TGF-β1*, *TSP-1*, *PAI-1*, and *TIMP-1* increased with 4 weeks of DMN treatment, while *HGF* gene expression decreased relative to the levels in normal control rats (Fig. 3C; normalized to GAPDH). Tissue protein levels showed suppression of HGF and increased expression of α-SMA (Supplementary Fig. S1D). Liver function was also affected, as shown by a decrease in serum albumin, and an increase in alanine transaminase (ALT) (Supplementary Fig. S1E). Thus, DMN-induced rat livers exhibited numerous molecular and functional features characteristic of fibrotic disease (Lee *et al.*, 2004).

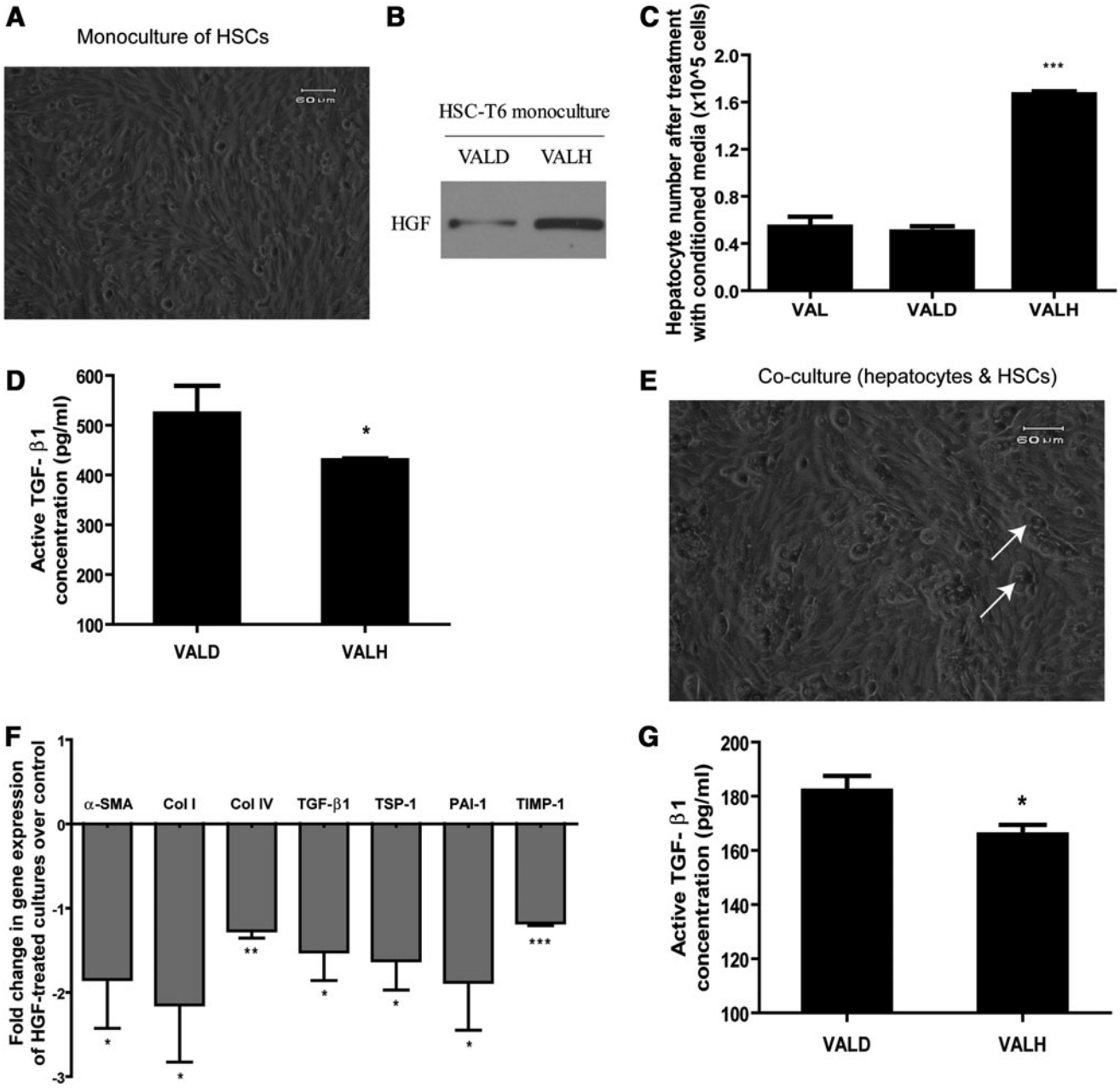

FIG. 2. Effects of vitamin A-liposome-HGF (VALH) treatment on HSC-T6 monoculture and HSC-T6/hepatocyte coculture. HSC-T6 monoculture **(A)** transfected with VALH complexes secreted higher levels of HGF **(B)**, and its hepatotrophic function was assessed by the induction of proliferation in primary rat hepatocytes after treatment with the conditioned media from these cells **(C)** and also decreased active transforming growth factor-β1 (TGF-β1) protein **(D)**. HSC-T6:hepatocyte coculture **(E)** (white arrows indicate hepatocytes) transfected with VALH complexes showed a decline in the gene expression of fibrotic markers compared to VALD-transfected coculture, normalized to *β-actin* **(F)** and a decline in active TGF-β1 **(G)**; $^{*}p < 0.05$, $^{**}p < 0.01$, $^{***}p < 0.001$ compared to VALD. VALD, vitamin A–coupled liposomes with pDsRed2 plasmid.

Vascular dysfunction in DMN-induced fibrotic livers

In DMN-induced rat livers, we also observed an alteration in the sinusoids. Sinusoidal endothelial fenestrae are nanoscale pores in sinusoidal endothelial cells (SECs) that facilitate exchange of substances between the blood and the hepatic parenchyma (Wisse *et al.*, 1985). Liver cirrhosis causes capillarization, whereby SECs lose their fenestrae and develop a basement membrane (Schaffner *et al.*, 1963; Martinez-Hernandez *et al.*, 1991). At 4 weeks of DMN induction, there was a drastic loss of endothelial fenestrations compared to the control rats, which had abundant fenestrae in sieve plate-like configurations (Fig. 3D). SEC defenestration was accompanied by increased expression of capillarization markers PECAM-1, vWF, and CD44 (Fig. 3E and F). DMN-induced perturbations of liver microvasculature would greatly reduce the exchange of substances between blood and the space of Disse. As reduced access to the space

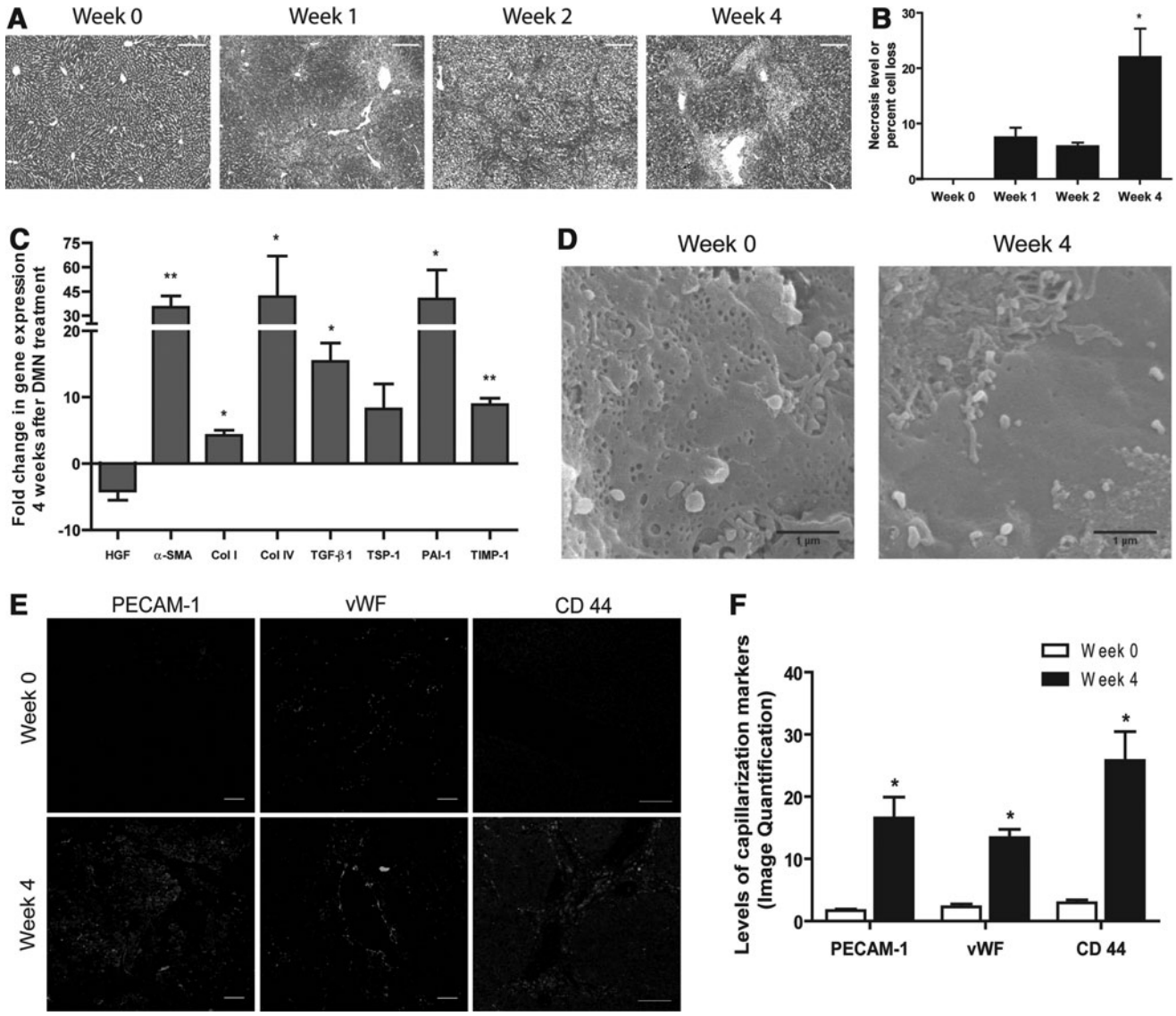

FIG. 3. Dimethylnitrosamine (DMN) administration induced fibrosis and caused defenestration of sinusoidal endothelial cells in rat livers. DMN administration led to an increase in necrosis of trichrome-stained liver tissue sections **(A** and **B)** ($p < 0.05$ compared to week 2) and an increase in gene expression of fibrotic markers at 4 weeks after DMN treatment compared to the control, normalized to GAPDH **(C)**. DMN-induced fibrosis also caused severe defenestration as seen in SEM images of hepatic sinusoids **(D)** and increases in the SEC capillarization marker proteins **(E** and **F)**; $^{*}p < 0.05$, $^{**}p < 0.01$ compared to control rats. Color images available online at www.liebertpub.com/hum

of Disse might impair the effective portal vein infusion of therapeutics (DeLeve, 2007), we chose to circumvent the blocked sinusoids for our therapy and used retrograde intrabiliary infusion to deliver the liposome/DNA complexes.

DMN-induced liver fibrosis regressed after VALH treatment

DMN-induced fibrotic rats, at the beginning of the fourth week, were administered a single dose of either liposome-pDsRed-HGF (Lip-HGF), VALD, or VALH complexes at a DNA dose of 200 μg through retrograde intrabiliary infusion at a constant rate of 0.2 ml/min (Supplementary Fig. S2A) and samples were collected at 1 and 7 days after therapeutic administration.

VALH treatment caused a decline in serum markers of liver fibrosis

To assess the changes in systemic liver fibrosis markers, we tested liver proteins ALT, aspartate aminotransferase (AST), and lactate dehydrogenase (LDH) in the blood serum. AST and LDH showed a significant decline with VALH treatment, compared with untargeted Lip-HGF-treated rats or compared with VALD-treated rats (Table 2). ALT showed spontaneous regression in all cohorts. The levels of hyaluronic acid (HA), a marker for hepatic endothelial cell damage, showed significant improvement with both targeted and untargeted delivery of HGF. The blood serum levels of active TGF-β1 also showed a decline with VALH treatment (Supplementary Fig. S2B; $p = 0.08$ between VALH

Table 2. Disease-Related Liver Proteins in the Blood Serum

	CTRL	*DMN*	*Lip-HGF*	*VALD*	*VALH*
ALT (U/L)	44.33 ± 1.33	86.67 ± 12.41	51.5 ± 14.80	53.5 ± 4.09	46.67 ± 3.67
AST (U/L)	149.67 ± 14.85	247.33 ± 19.36	167.75 ± 4.48	182 ± 5.93	123.5 ± 14.43[a,b]
LDH (kU/L)	148 ± 1.63	143 ± 8.96	291.5 ± 21.88	136.75 ± 10.82	131.33 ± 13.87[c]
HA (ng/ml)	26.2 ± 8.95	46.45 ± 29.58	27.61 ± 5.73	39.86 ± 16.57	18.54 ± 5.55[b]

[a] $p < 0.05$ compared to Lip-HGF.
[b] $p < 0.05$ compared to VALD.
[c] $p < 0.01$ compared to Lip-HGF.
ALT, alanine transaminase; AST, aspartate aminotransferase; DMN, dimethylnitrosamine; LDH, lactate dehydrogenase; Lip-HGF, liposomes with pDsRed2-HGF; HA, hyaluronic acid; VALD, vitamin A–coupled liposomes with pDsRed2 plasmid; VALH, vitamin A–coupled liposomes with pDsRed2-HGF plasmid.

and Lip-HGF groups). In summary, targeted delivery of *HGF* transgene showed significant improvement in multiple markers compared to untargeted *HGF* gene delivery.

Localized delivery of HGF transgene to areas expressing α-SMA

To investigate whether the *HGF* transgene had been delivered selectively to fibrotic foci, we observed the relative localization of DsRed2/HGF with either α-SMA or collagen by double immunofluorescence staining. We found that in VALH-treated rat livers, as early as 24 hr, the DsRed2-HGF protein was strongly colocalized with α-SMA-positive cells in the collagen-rich fibrotic foci (Fig. 4A and B; Supplementary Fig. S2C). VALH treatment also increased *HGF* transgene expression (Supplementary Fig. S2D) in DMN-induced fibrotic rat livers.

VALH treatment improved structural markers of liver fibrosis

Seven days after treatment, VALH-treated rat livers showed reduced necrosis levels (Fig. 4C and D) compared with nontargeted delivery of HGF. Scanning electron microscopy showed that both cohorts with HGF treatment exhibited normal fenestration in sinusoids (Fig. 4E), regardless of liposomal targeting, whereas VALD and DMN cohorts showed defenestration and microvascular disruption, which correlated well with serum HA levels. SHG imaging of the treated rat liver sections showed a decline in collagen levels (Supplementary Fig. S3A; SHG imaging).

VALH treatment decreased the levels of α-SMA-positive myofibroblasts, TGF-β1, and collagen I at the fibrotic foci

We further investigated whether the HSC-targeted delivery of the *HGF* transgene decreased the HSC-specific fibrotic markers by measuring protein markers specifically at the portal regions as well as the capsular regions that represent HSC-rich fibrotic foci. VALH treatment significantly increased the HGF protein levels and significantly reduced the α-SMA protein levels when compared to other treatments (Fig. 5A–C; Supplementary Fig. S3B). Fibrotic markers such as TGF-β1 (Fig. 5A and D) and collagen I (Fig. 5A and E) decreased significantly in the VALH-treated rats compared with other treatments. Thus, VALH treatment effectively targeted the fibrotic foci, decreased α-SMA-positive cells, and caused regression of liver fibrosis.

Discussion

During fibrosis progression, the liver shows varied regional susceptibility to injury and toxins due to architectural complexities, protein gradients, and oxygen levels (Matsuzaki *et al.,* 1997; Heinloth *et al.,* 2004; Anderson and Borlak, 2008). Regardless of different etiologies of liver fibrosis, HSCs become activated, proliferative, migrate to fibrotic regions, and become highly abundant in the fibrotic foci. Targeting HSCs is therefore a strategy to deliver therapeutics specifically to fibrotic foci, thereby enhancing the local availability of the therapeutic at the disease sites (Shek *et al.,* 2004; Iredale, 2008; Fallowfield, 2011; Poelstra and Schuppan, 2011). Localized targeting may be particularly important in liver fibrosis because of low diffusion to the fibrotic foci caused by high collagen deposition and poor microcirculation (Wang *et al.,* 2009). We used Vitamin A–coupled liposomes to specifically target HSCs (Sato *et al.,* 2008) and found that specific targeting increased localized expression of the *HGF* transgene at the fibrotic foci (Fig. 4A and B).

Although HSCs have been identified as a target for treating liver fibrosis and are abundant at the fibrotic foci, the immense synthetic/metabolic capability of myofibroblastic HSCs has not yet been harnessed to facilitate disease regression via hepatic regeneration. Previous therapies have targeted HSCs to block their fibrogenic functions, such as matrix production (Adrian *et al.,* 2007; Sato *et al.,* 2008; Son *et al.,* 2009); but we have targeted HSCs to induce the production of HGF and hepatic regeneration. Our approach targeted HGF to the fibrotic foci, where regenerative capacity could be lacking.

Another important role of HGF is its antifibrotic effects. We have shown that transfection of fibrotic cell cultures (HSC-T6 monoculture and coculture with hepatocytes) with the VALH complexes increased the expression of functional HGF and significantly decreased the expression of fibrotic markers at both the gene and protein levels (Fig. 2). In DMN-induced fibrotic rats, we observed extensive hepatocyte damage and high levels of α-SMA and collagen-producing myofibroblasts and severe disruption of the hepatic sinusoids (due to loss of endothelial fenestration and increased SEC capillarization) (Fig. 3; Supplementary Fig. S1). The administration of HSC-targeted therapeutic complexes by retrograde intrabiliary infusion allowed us to overcome the

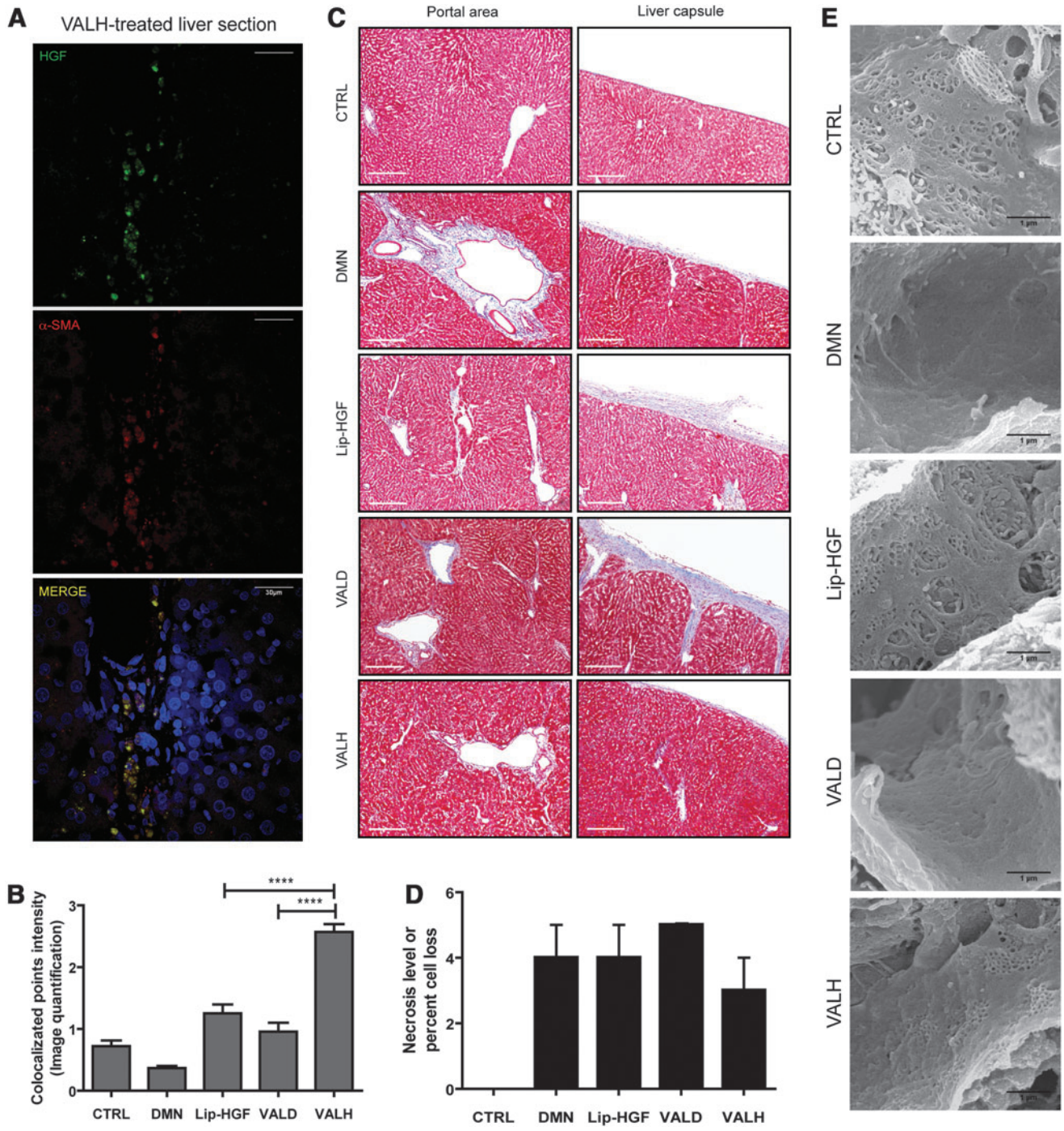

FIG. 4. VALH treatment reduced hepatocellular loss, collagen deposition, and defenestration in DMN-induced rat livers. At 24 hr after VALH treatment, the HGF expression significantly increased within α-SMA-positive-myofibroblasts **(A** and **B)** demonstrating targeting for activated HSCs and fibrotic foci. Seven days after VALH treatment, DMN-induced fibrotic rats showed a decline in the deposited collagen levels **(C)** as measured by Masson's Trichrome staining and necrosis levels **(D)**. Endothelial fenestrations were restored in both HGF-treated groups, Lip-HGF and HGF compared to VALD treatment **(E)**. ****$p < 0.0001$.

issue of sinusoidal resistance and effectively deliver them within close proximity of the fibrotic foci. In addition to effective delivery, the HGF-treated cohorts demonstrated re-fenestration of the hepatic sinusoids and restoration of the fenestrated endothelium structure (Fig. 4E).

It is worth noting that we have previously examined the potential damage and toxicity of bile duct infusion to the liver parenchyma and biliary tree in rats by biochemical analysis of blood samples and histochemical examination of the livers that received intrabiliary infusion of plasmid DNA

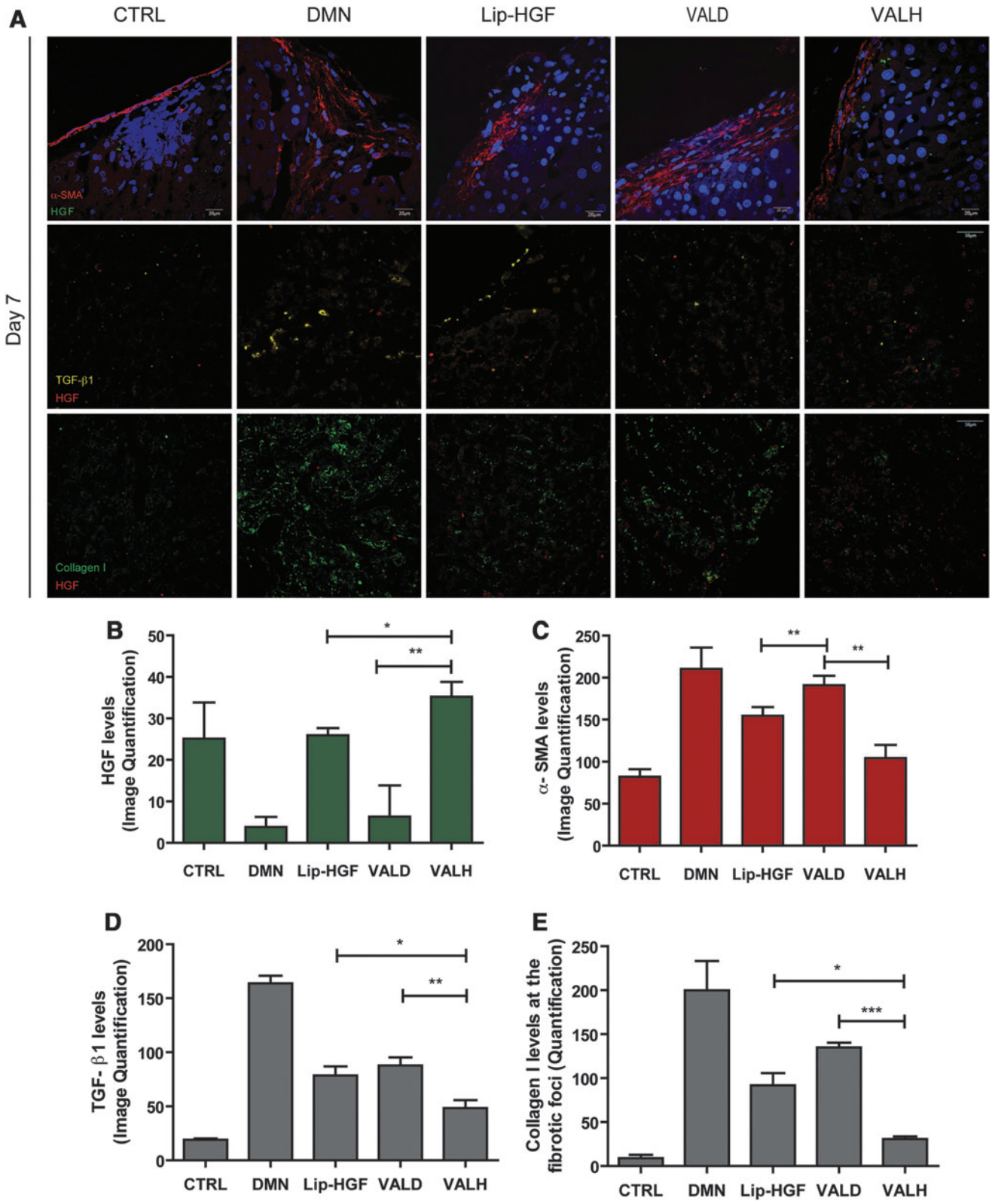

FIG. 5. Increased expression of HGF at the fibrotic foci (portal and capsular) correlates with reduction in fibrotic markers. Confocal micrographs of liver tissue sections stained for α-SMA (red) and HGF (green) **(A)**. The rats treated with VALH complexes had higher levels of HGF protein **(B)** and lower levels of α-SMA **(C)**, TGF-β1 **(D)**, and Collagen I **(E)** at the fibrotic foci. *$p < 0.05$, **$p < 0.01$, ***$p < 0.001$.

(Dai *et al.*, 2006; Jiang *et al.*, 2007). The studies showed that there is a slight increase in serum AST and ALT activities at 1 day after infusion of plasmid DNA, followed by rapid decrease to the background level by day 3. The histopathological examination on the liver sections from a naked DNA-infused rat showed minimal changes with patchy mild bile ductular proliferation and mild reactive changes in the biliary epithelium, and most of the portal tracks were essentially normal. These results concluded that the tissue responses in the liver were very mild and transient (Dai *et al.*, 2006).

VALH complex treatment in DMN-induced fibrotic rats caused an increase in *HGF* transgene expression (Supplementary Fig. S2D) and a clear decline in the fibrotic markers as compared to the other treatment groups (Table 1 and Fig. 4; Supplementary Fig. S3). Vitamin A–based targeting greatly increased expression levels of the delivered transgene in the fibrotic foci relative to other treatments. This was accompanied by a reduction in the protein levels of fibrotic markers α-SMA, TGF-β1, and collagen I (Fig. 5). VALH treatment thus effectively increased local expression of HGF at the fibrotic foci and reduced the levels of fibrotic markers. When the *HGF* transgene is targeted specifically to HSCs via Vitamin A–coupled liposomes and is well localized within the fibrotic foci, it can effectively ameliorate hepatocellular damage, reduce adverse effects on healthy nonspecific cells around the foci, and cause marked antifibrotic effects on HSC activation or fibrosis progression. This *HGF* gene therapy targeted specifically to HSCs can be further developed to effectively treat fibrosis-related liver diseases.

Acknowledgments

We thank Inn Chuan Ng, Abhishek Anathanarayanan, Wuzheng Xia, Rui Rui Jia, and other members of the Laboratory of Cellular and Tissue Engineering in the National University of Singapore for technical assistance and scientific discussion. This study was supported by grants from Singapore-MIT Alliance Computational and Systems Biology Flagship Project (C-382-641-001-091); Mechanobiology Institute of Singapore (R-714-001-003-271); Janssen Sourcing Pte Ltd (R-185-000-182-592); SMART BioSyM program; and Institute of Bioengineering and Nanotechnology, Agency for Science, Technology and Research, Singapore.

Author Disclosure Statement

The authors declare that no competing financial interests exist.

References

Adrian, J.E., Poelstra, K., Scherphof, G.L., *et al*. (2007). Effects of a new bioactive lipid-based drug carrier on cultured hepatic stellate cells and liver fibrosis in bile duct-ligated rats. *Journal of Pharmacology and Experimental Therapeutics* 321, 536–543.

Anderson, N., and Borlak, J. (2008). Mechanisms of toxic liver injury. In *Hepatotoxicity: From Genomics to In Vitro and In Vivo Models*. Sahu SC, ed. (John Wiley & Sons, Hoboken, NJ). *pp.* 191–286.

Bataller, R., and Brenner, D.A. (2005). Liver fibrosis. J. Clin. Invest. 115, 209–218.

Budinger, G.R., Mutlu, G.M., Eisenbart, J., *et al*. (2006). Proapoptotic Bid is required for pulmonary fibrosis. Proc. Natl. Acad. Sci. U.S.A. 103, 4604–4609.

Dai, H., Jiang, X., Tan, G.C., *et al*. (2006). Chitosan-DNA nanoparticles delivered by intrabiliary infusion enhance liver-targeted gene delivery. Int. J. Nanomedicine 1, 507–522.

DeLeve, L.D. (2007). Hepatic microvasculature in liver injury. Semin. Liver Dis. 27, 390–400.

Ebrahimkhani, M.R., Oakley, F., Murphy, L.B., *et al*. (2011). Stimulating healthy tissue regeneration by targeting the 5-HT(2)B receptor in chronic liver disease. Nat. Med. 17, 1668–1673.

Fallowfield, J.A. (2011). Therapeutic targets in liver fibrosis. Am. J. Physiol. Gastrointest. Liver Physiol. 300, G709–G715.

Heinloth, A.N., Irwin, R.D., Boorman, G.A., *et al*. (2004). Gene expression profiling of rat livers reveals indicators of potential adverse effects. Toxicol. Sci. 80, 193–202.

Hu, Z., Evarts, R.P., Fujio, K., *et al*. (1993). Expression of hepatocyte growth factor and c-met genes during hepatic differentiation and liver development in the rat. Am. J. Pathol. 142, 1823–1830.

Inoue, T., Okada, H., Kobayashi, T., *et al*. (2003). Hepatocyte growth factor counteracts transforming growth factor-beta1, through attenuation of connective tissue growth factor induction, and prevents renal fibrogenesis in 5/6 nephrectomized mice. FASEB J. 17, 268–270.

Iredale, J. (2008). Recent developments in targeting liver fibrosis. Clin. Med. 8, 29–31.

Ishiki, Y., Ohnishi, H., Muto, Y., *et al*. (1992). Direct evidence that hepatocyte growth factor is a hepatotrophic factor for liver regeneration and has a potent antihepatitis effect in vivo. Hepatology 16, 1227–1235.

Jiang, D., Jiang, Z., Han, F., *et al*. (2008). HGF suppresses the production of collagen type III and alpha-SMA induced by TGF-beta1 in healing fibroblasts. Eur. J. Appl. Physiol. 103, 489–493.

Jiang, X., Dai, H., Ke, C.Y., *et al*. (2007). PEG-b-PPA/DNA micelles improve transgene expression in rat liver through intrabiliary infusion. J. Control Release 122, 297–304.

Kanemura, H., Iimuro, Y., Takeuchi, M., *et al*. (2008). Hepatocyte growth factor gene transfer with naked plasmid DNA ameliorates dimethylnitrosamine-induced liver fibrosis in rats. Hepatol. Res. 38, 930–939.

Kisseleva, T., and Brenner, D.A. (2007). Role of hepatic stellate cells in fibrogenesis and the reversal of fibrosis. J. Gastroenterol. Hepatol. 22, S73–S78.

Lee, M.H., Yoon, S., and Moon, J.O. (2004). The flavonoid naringenin inhibits dimethylnitrosamine-induced liver damage in rats. Biol. Pharm. Bull. 27, 72–76.

Martinez-Hernandez, A., and Martinez, J. (1991). The role of capillarization in hepatic failure: studies in carbon tetrachloride-induced cirrhosis. Hepatology 14, 864–874.

Matsuzaki, S., Onda, M., Tajiri, T., and Kim, D.Y. (1997). Hepatic lobar differences in progression of chronic liver disease: correlation of asialoglycoprotein scintigraphy and hepatic functional reserve. Hepatology 25, 828–832.

Narmada, B.C., Chia, S.M., Tucker-Kellogg, L., and Yu, H. (2012). HGF regulates the activation of TGF-beta1 in rat hepatocytes and hepatic stellate cells. J. Cell. Physiol. 228, 393–401.

Olsen, A.L., Bloomer, S.A., Chan, E.P., *et al*. (2011). Hepatic stellate cells require a stiff environment for myofibroblastic differentiation. Am. J. Physiol. Gastrointest. Liver Physiol. 301, G110–G118.

Otsuka, M., Baru, M., Delrivière, L., *et al.* (2000). In vivo liver-directed gene transfer in rats and pigs with large anionic multilamellar liposomes: routes of administration and effects

of surgical manipulations on transfection efficiency. Journal of Drug Targeting 8, 267–279.
Poelstra, K., and Schuppan, D. (2011). Targeted therapy of liver fibrosis/cirrhosis and its complications. J. Hepatol. 55, 726–728.
Sato, Y., Murase, K., Kato, J., *et al*. (2008). Resolution of liver cirrhosis using vitamin A-coupled liposomes to deliver siRNA against a collagen-specific chaperone. Nat. Biotechnol. 26, 431–442.
Schaffner, F., and Poper, H. (1963). Capillarization of hepatic sinusoids in man. Gastroenterology 44, 239–242.
Schuppan, D., and Pinzani, M. (2012). Antifibrotic therapy: lost in translation? J. Hepatol. 56, S66–74.
Scotton, C.J., and Chambers, R.C. (2007). Molecular Targets in Pulmonary Fibrosis*. Chest 132, 1311–1321.
Seglen, P.O. (1976). Preparation of isolated rat liver cells. Methods Cell. Biol. 13, 29–83.
Shek, F.W., and Benyon, R.C. (2004). How can transforming growth factor beta be targeted usefully to combat liver fibrosis? Eur. J. Gastroenterol. Hepatol. 16, 123–126.
Son, G., Hines, I.N., Lindquist, J., *et al*. (2009). Inhibition of phosphatidylinositol 3-kinase signaling in hepatic stellate cells blocks the progression of hepatic fibrosis. Hepatology 50, 1512–1523.
Tai, D.C., Tan, N., Xu, S., *et al*. (2009). Fibro-C-Index: comprehensive, morphology-based quantification of liver fibrosis using second harmonic generation and two-photon microscopy. J. Biomed. Opt. 14, 044013.
van't Veer, M.B., Brooijmans, A.M., Langerak, A.W., *et al*. (2006). The predictive value of lipoprotein lipase for survival in chronic lymphocytic leukemia. Haematologica 91, 56–63.
Wang, Z.X., Wang, Z.G., Ran, H.T., *et al*. (2009). The treatment of liver fibrosis induced by hepatocyte growth factor-directed, ultrasound-targeted microbubble destruction in rats. Clin. Imaging 33, 454–461.
Wisse, E., De Zanger, R.B., Charels, K., *et al*. (1985). The liver sieve: considerations concerning the structure and function of endothelial fenestrae, the sinusoidal wall and the space of Disse. Hepatology 5, 683–692.
Wisse, E., Braet, F., Duimel, H., *et al*. (2010). Fixation methods for electron microscopy of human and other liver. World J. Gastroenterol. 16, 2851–2866.

Address correspondence to:
Prof. Hanry Yu
Department of Physiology
Block MD11, #04-01A
National University of Singapore
10 Medical Drive
Singapore 117597
Singapore

E-mail: hanry_yu@nuhs.edu.sg

Hai-Quan Mao
Department of Materials Science and Engineering
113 Maryland Hall
Johns Hopkins University
3400 North Charles Street
Baltimore, MD 21218

E-mail: hmao@jhu.edu

Received for publication August 27, 2012;
accepted after revision March 10, 2013.

Published online: March 25, 2013.